Self-Assembly

Deutsche Ausgabe: DOI: 10.1002/ange.201603409
Internationale Ausgabe: DOI: 10.1002/anie.201603409

N-Substituted Dicyanomethylphenyl Radicals: Dynamic Covalent Properties and Formation of Stimuli-Responsive Cyclophanes by Self-Assembly

Toshiyuki Kobashi, Daisuke Sakamaki, and Shu Seki**

Abstract: *Dynamic covalent bonds and their chemistry have been of particular interest both from a fundamental and materials science aspect. Demonstrated herein is that triphenylamine (TPA) and carbazole (Cz), substituted with a dicyanomethyl radical, are useful motifs for dynamic covalent chemistry as they have the appropriate bond strength between monomer units as well as high stability and synthetic simplicity. TPA and Cz units substituted by two dicyanomethyl radicals formed macrocyclic oligomers classified as novel types of azacyclophanes, and in particular, the TPA-based diradical gave a cyclic dimer in almost quantitative yield. The cyclic oligomers exhibited thermo- and mechanochromic behavior resulting from the generation of radical species by intermonomer C−C bond cleavage.*

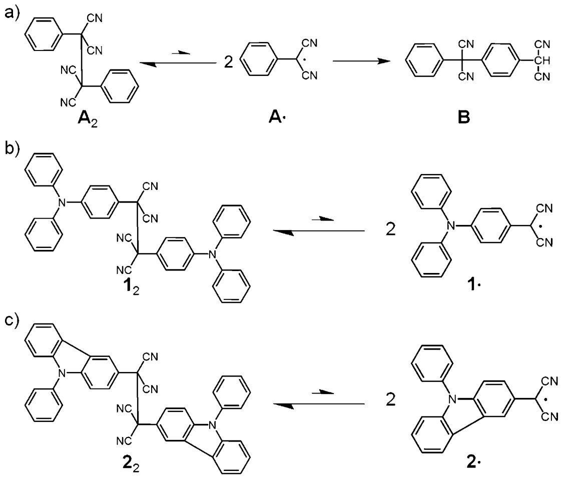

Scheme 1. a) Equilibrium between $\mathbf{A}_2$ and $\mathbf{A}^{\bullet}$, and isomerization to **B**. b) Equilibrium between $\mathbf{1}_2$ and $\mathbf{1}^{\bullet}$, c) Equilibrium between $\mathbf{2}_2$ and $\mathbf{2}^{\bullet}$.

Dynamic covalent chemistry (DCC) has been intensively studied because of its potential for selective construction of the thermodynamically most stable product by self-assembly processes.[1–4] As a motif of DCC, organic radicals are promising compounds because of the simplicity of the reaction equilibrium, that is, it does not involve catalysts or byproducts.[5–14] We have focused on aryldicyanomethyl radicals because of their symmetric and sterically unhindered structures, which do not give diastereomers upon dimerization. In 1966, Hartzler reported that 1,2-diphenyl-1,1,2,2-tetracyanoethane ($\mathbf{A}_2$), which is regarded as the dimer of the phenyldicyanomethyl radical ($\mathbf{A}^{\bullet}$), is in equilibrium with $\mathbf{A}^{\bullet}$ in solution.[5] However, $\mathbf{A}^{\bullet}$ was easily decomposed irreversibly to form **B** because of the high reactivity at its *para*-position (Scheme 1 a). It was also reported that the introduction of a substituent such as a Me, Cl, and NO_2 group at the *para*-position of the dicyanomethyl group prohibited such an isomerization reaction.[6–8] However, the equilibrium strongly favored the dimeric form for such cases at room temperature. To realize the selective formation of thermodynamic products by DCC, a sufficiently fast equilibration is required.[1] In this context, the stabilization of the radical state by promoting spin-delocalization would be key to the design of radical-based DCC systems. The introduction of an electron-donor group at the position *para* to the radical center can stabilize the radical form by enabling spin-delocalization onto the donor unit as well as blocking the undesired reactions at the *para* position.

In this study, we report that triphenylamine (TPA) and carbazole (Cz) derivatives substituted bearing a dicyanomethyl radical are useful motifs for DCC with exceptional stability and increased dynamicity (Schemes 1 b and c). The details of the dissociation and recombination phenomena of these radicals were investigated by spectroscopic measurements, and we also demonstrate the formation of macrocyclic oligomers by self-assembly of the monomers having two radicals.

The TPA and Cz dimers, $\mathbf{1}_2$ and $\mathbf{2}_2$, respectively, were prepared by the oxidation of the precursors of the corresponding radicals[5] (Schemes 1 b and c; see Scheme S1 in the Supporting Information), and their structures were unambiguously determined by X-ray single crystal analysis[15] (see Figure S3). The C−C bond between monomers were significantly longer (1.616 Å for $\mathbf{1}_2$ and 1.626 Å for $\mathbf{2}_2$) than usual C(sp^3)−C(sp^3) bonds (1.54 Å).

The solutions of $\mathbf{1}_2$ and $\mathbf{2}_2$ showed green and faint blue colors, respectively, even at room temperature, thus suggesting the existence of the dissociated radical species. To investigate the monomer–dimer equilibria in solution, UV/Vis-NIR absorption spectra were measured in toluene at temperatures between 293 and 363 K (Figure 1). For $\mathbf{1}_2$, the low-energy absorption band around $\lambda = 700$ nm, which could be ascribed to the dissociated radical $\mathbf{1}^{\bullet}$ by time-dependent

---

[*] T. Kobashi, Dr. D. Sakamaki, Prof. Dr. S. Seki
Department of Molecular Engineering
Graduate School of Engineering, Kyoto University
Nishikyo-ku, Kyoto 615-8510 (Japan)
E-mail: sakamaki@moleng.kyoto-u.ac.jp
seki@moleng.kyoto-u.ac.jp

Supporting information and the ORCID identification number(s) for the author(s) of this article can be found under http://dx.doi.org/10.1002/anie.201603409.

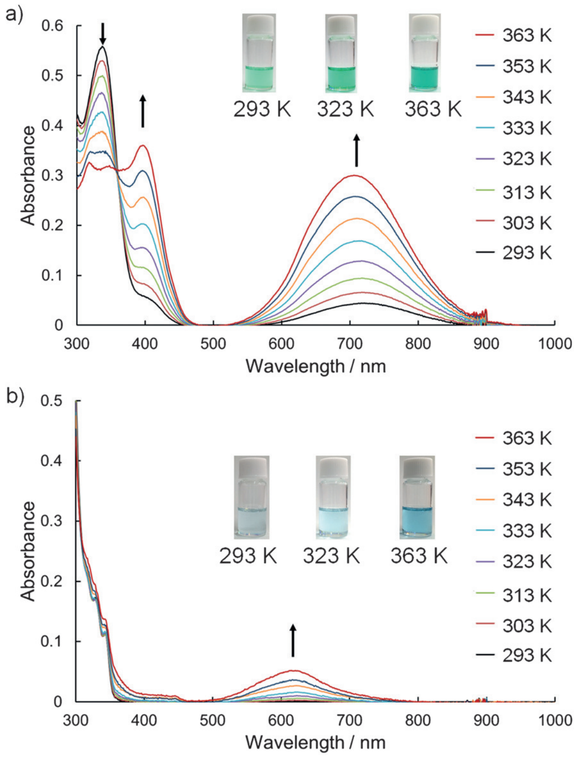

Figure 1. Temperature dependence of the absorption spectra and the color changes of $\mathbf{1}_2$ (a) and $\mathbf{2}_2$ (b) in toluene (2×10^{-5} M) under air.

density functional theory (TD-DFT) calculations (see Figure S11), was clearly observed even at 293 K, in addition to the strong peak at $\lambda = 337$ nm which corresponds to the absorption of the TPA moieties. Upon increasing the temperature, the intensities of the low-energy band increased, thus suggesting an increase in the amount of the dissociated radical in the solution. The existence of an isosbestic point at $\lambda =$ 359 nm demonstrates a dimer–monomer equilibrium without any decomposition reactions, as seen in the case of $\mathbf{A}_2$, and it is also supported by recovery of the initial spectrum by cooling to 293 K (see Figure S13). For $\mathbf{2}_2$, a similar temperature dependence was observed. The low-energy band corresponding to $\mathbf{2}^{\bullet}$ was seen around $\lambda = 620$ nm, slightly blue-shifted compared to that of $\mathbf{1}_2$, and the TD-DFT calculations reproduced this trend (see Figure S12). The intensity of the radical bands was relatively weaker, thus suggesting that $\mathbf{2}_2$ is harder to dissociate than $\mathbf{1}_2$. The absorption spectra of the radical species did not change, even after the addition of 2,2-diphenyl-1-picrylhydrazyl (DPPH) as a radical scavenger for several hours, thus showing the exceptionally high stability of the dissociated radicals (see Figure S15).

The toluene solution of $\mathbf{1}_2$ showed a clear ESR and a broadened NMR spectrum at room temperature because of an appreciable amount of radical species. The ESR intensity gradually decreased with decreasing temperature and almost disappeared at 223 K, at which point clear NMR signals were observed (Figures S4–S6). In contrast, the toluene solution of $\mathbf{2}_2$ gave a significantly weaker ESR and resolved NMR spectra at room temperature, and is in accord with the results of the absorption measurement.

We estimated the enthalpy and entropy changes for the dissociation (ΔH_{diss} and ΔS_{diss}) of $\mathbf{1}_2$ and $\mathbf{2}_2$ from the temperature dependence of the dissociation equilibrium constant (see the Supporting Information).[10] The value of ΔH_{diss} corresponds to the bond dissociation energy (BDE) for the C–C bond between monomers. The calculated parameters are summarized in Table 1. The BDE of $\mathbf{1}_2$ was significantly smaller than that of the related dimers of carbon-centered radicals, thus suggesting the higher dynamic character of this system.[10–12]

Table 1: Related parameters for bond dissociation of $\mathbf{1}_2$ and $\mathbf{2}_2$.

	$\lambda_{\max}$ of the dissociated radical [nm]	ε at $\lambda_{\max}$ [$\mathrm{M}^{-1}\,\mathrm{cm}^{-1}$]	ΔH_{diss} [$\mathrm{kJ\,mol^{-1}}$]	ΔS_{diss} [$\mathrm{J\,K^{-1}\,mol^{-1}}$]
$\mathbf{1}_2$	712	15 500	55.0	67.8
$\mathbf{2}_2$	620	16 200	75.2	86.3

The origin of the difference of the BDE between $\mathbf{1}_2$ and $\mathbf{2}_2$ could be explained by the difference of the spin density distribution of $\mathbf{1}^{\bullet}$ and $\mathbf{2}^{\bullet}$. For $\mathbf{1}^{\bullet}$, the spin density on the central carbon atom of the dicyanomethyl group is smaller than that compared to $\mathbf{2}^{\bullet}$, and the spin density on the amino nitrogen atom is larger compared to that of $\mathbf{2}^{\bullet}$ (see Figure S17). This result could be ascribed to the higher electron-donor ability of TPA than Cz. We also checked other substituents (OMe, Me, Cl, and NO_2) and found that the spin density on the bridgehead carbon atom increased in the following order: TPA < Cz < OMe < Me < Cl < NO_2, thus indicating that the strong electron-donor group at the *para*-position decreases the spin density on the bridgehead carbon atom and consequently weakens the bridging C–C bond in the dimeric form. The present results demonstrate the introduction of donor groups as an effective way to tune the strength of the dynamic covalent bonds based on the dissociation/recombination reaction of radicals.

It is expected that a molecule having multiple radical centers as reactive sites can form various self-assembled structures depending on the topology of the monomer, such as periodic networks[16,17] or macrocyclic structures.[18–21] As a first step, we tried to introduce yet another dicyanomethyl radical to $\mathbf{1}^{\bullet}$ and $\mathbf{2}^{\bullet}$. TPA and Cz having two appended dicyanomethyl radicals, **3** and **4**, respectively, can possibly construct linear chain structures or cyclic oligomers (Scheme 2). The precursors of **3** and **4** with two hydrogen atoms were oxidized by potassium ferricyanide or DDQ. For the oxidation of $\mathbf{3}_{\mathbf{2H}}$, the generation of one colorless spot was observed by TLC, and the product was obtained in nearly quantitative yield as a pale yellow powder after silica gel chromatography. For the oxidation of $\mathbf{4}_{\mathbf{2H}}$, two colorless products were obtained in addition to an insoluble blue solid.

The product from $\mathbf{3}_{\mathbf{2H}}$ showed the ^{1}H NMR signals for only one TPA unit, thus indicating the formation of a highly symmetric cyclic oligomer. By X-ray single-crystal analysis, this compound was shown to be a cyclic dimer ($\mathbf{3}_2$; Figure 2).[15] The two C–C bonds between monomers were

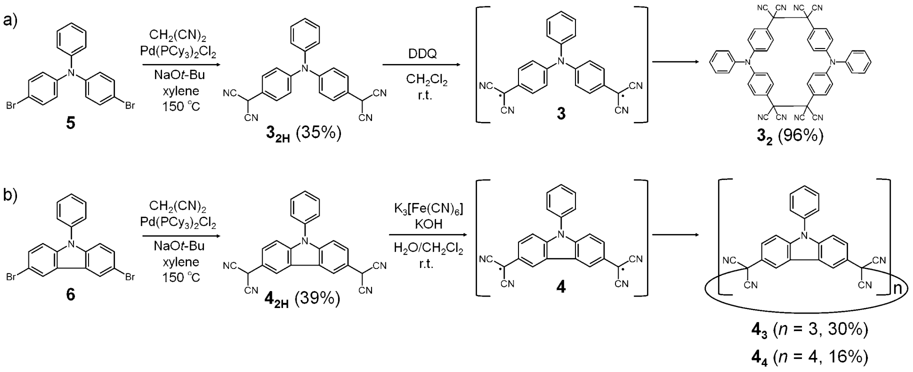

Scheme 2. Synthesis of the oligomers of **3** and **4**. DDQ = 2,3-dichloro-5,6-dicyano-1,4-benzoquinone.

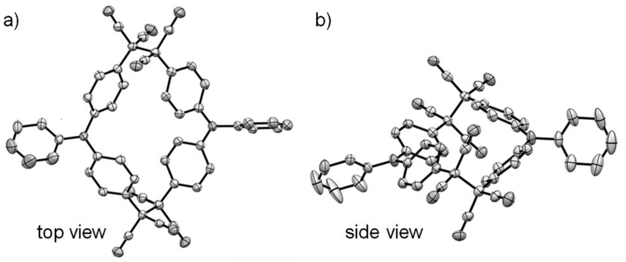

Figure 2. ORTEP representation of $\mathbf{3_2}$. a) Top view. b) Side view. Hydrogen atoms are omitted for clarity. Thermal ellipsoids are set at 50% probability.

also longer (1.634 and 1.643 Å) than typical C(sp^3)–C(sp^3) bonds, thus suggesting the weakness of these bonds and the possibility of the bond cleavage by an external stimuli. The phenyl rings incorporated in the macrocycle were largely twisted around the central nitrogen atoms to reduce the strain derived from its macrocyclic structure. The effect of the structural constraints were also seen in the ^{1}H NMR spectra of these phenyl rings. The inner and outer protons were observed as different signals, thus indicating the restricted rotation of these phenyl rings (see Figure S8).

The two products from $\mathbf{4_{2H}}$ were suggested to be a trimer ($\mathbf{4_3}$) and a tetramer ($\mathbf{4_4}$) by electrospray ionization mass spectrometry (ESI-MS) measurements. The insoluble blue solid obtained as byproduct was thought to be the higher oligomer or polymer of **4** with intact radicals at their ends. The structure of $\mathbf{4_3}$ was unequivocally determined to be a cyclic trimer by single-crystal X-ray analysis (Figure 3).[15] Interestingly, there exists two enantiomer in a crystal. One has a right-handed helicity and is regarded as a *P* isomer, and the other has a left-handed helicity and is regarded as a *M* isomer. The C–C bond length between monomers are also elongated (1.608–1.639 Å). Unfortunately, we could not obtain single crystals of $\mathbf{4_4}$. However, $\mathbf{4_4}$ is thought to have a highly symmetric or flexible structure in solution judging from its ^{1}H NMR spectrum which shows only one set of protons for the 9-phenylcarbazole unit.

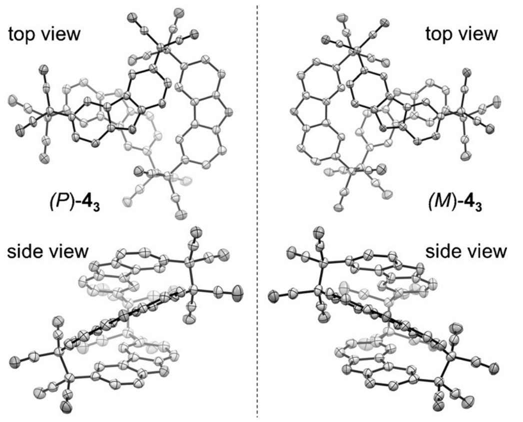

Figure 3. ORTEP representation of the *P*- and *M*-isomers of $\mathbf{4_3}$. Phenyl groups and hydrogen atoms are omitted for clarity. Thermal ellipsoids are set at 50% probability.

We could not detect the generation of the cyclic dimer $\mathbf{4_2}$, and a DFT calculation was performed on $\mathbf{4_2}$ to address this issue. In the optimized structure of $\mathbf{4_2}$, the C–C bonds between monomers were predicted to be abnormally long (1.683 and 1.686 Å), probably because of the large strain coming from the slightly bent Cz skeletons, and thus $\mathbf{4_2}$ may be thermodynamically disfavored (see Figure S18).

Whereas **3** almost exclusively gave $\mathbf{3_2}$, **4** gave at least two kinds of cyclic oligomers, as well as insoluble higher oligomers. The result can be explained by the following two reasons: 1) the higher oligomers of **4** were precipitated and could not participate in the equilibrium because of their low solubility; 2) the relatively more robust C–C bonds between Cz-based radicals than those of TPA-based radicals increased activation energies for the dissociation reactions, and gave some products as a result of kinetic trapping.[2]

The cyclic oligomers $\mathbf{3_2}$, $\mathbf{4_3}$, and $\mathbf{4_4}$ showed no radical absorption bands in solution at room temperature. The absorption spectra of $\mathbf{4_3}$ and $\mathbf{4_4}$ did not change even after heating at 373 K in toluene. Interestingly, for $\mathbf{3_2}$, we could observe the appearance of two kinds of weak absorption bands around $\lambda = 660$ nm and 850 nm upon heating (see Figure S20). The peak wavelength of the former band is close to that of $\mathbf{1^{\bullet}}$, and therefore this band could be due to the acyclic dimer of **3** having dicyanomethyl radicals at both ends. In contrast, the broad band around $\lambda = 850$ nm could probably be attributed to the monomer **3** itself, judging from the TD-DFT calculation for **3** (see Figure S21). Compared to acyclic dimers $\mathbf{1_2}$ and $\mathbf{2_2}$, the dissociation of the cyclic oligomers was remarkably suppressed in the solution, thus reflecting the smaller ΔS_{diss} than the acyclic oligomers.

Next, we checked the bond dissociation in the solid state by thermal energy. The drop cast films of $\mathbf{3_2}$, $\mathbf{4_3}$, $\mathbf{4_4}$ were formed on quartz plates and the plates were gradually heated on a hot plate. The colorless film of $\mathbf{3_2}$ started to turn green at around 100 °C, and the film of $\mathbf{4_3}$ and $\mathbf{4_4}$ turned blue at around 140 °C. The colors of the TPA and Cz oligomers after heating

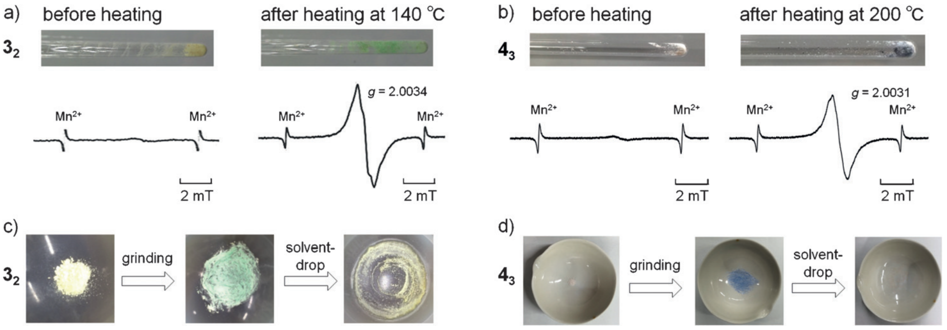

Figure 4. Pictures of a sample of $\mathbf{3_2}$ (a) and $\mathbf{4_3}$ (b) in an ESR tube and ESR spectra of before heating and after heating. Pictures of mechanochromic behavior of a powder sample of $\mathbf{3_2}$ (c) and $\mathbf{4_3}$ (d) and recovery of color by adding drops of CH_2Cl_2.

coincided with the colors of the corresponding monoradical $\mathbf{1}^{\bullet}$ and $\mathbf{2}^{\bullet}$, respectively. The colors of the films remained almost unchanged after cooling down to room temperature for a few days, but immediately recovered their original colors by dropping solvent onto the plate and then drying. These results indicate that the C–C bond recombination is restricted in the solid state because of constrained molecular flexibility. We measured the ESR spectra of the powder samples of $\mathbf{3_2}$ and $\mathbf{4_3}$ before and after heating. Figures 4a,b show the pictures of solid $\mathbf{3_2}$ and $\mathbf{4_3}$ in an ESR tube before and after heating, and then when cooled to room temperature. Whereas $\mathbf{3_2}$ and $\mathbf{4_3}$ showed no ESR signal before heating, the colored samples after heating showed clear ESR signals. The percentages of the dissociated radicals were estimated to be less than 1 % for both of $\mathbf{3_2}$ and $\mathbf{4_3}$, even after heating to 200 °C, according to the ESR signal intensities.

Similar color changes were observed after grinding the powders with a mortar and pestle. All the cyclic oligomers exhibited color changes from pale yellow to green (for $\mathbf{3_2}$) and from white to blue (for $\mathbf{4_3}$ and $\mathbf{4_4}$) after grinding (Figure 4c,d), as confirmed by the diffuse reflectance spectroscopy measurements (see Figures S23 and S24). The ground powders exhibited ESR signals similar to those of the heated samples.[12–14] The recovery of their colors by solvent treatment were also observed, thus showing the dynamic covalent properties of these cyclophanes.

In conclusion, we have shown that the TPA and Cz derivatives having appended dicyanomethyl radicals are effective and tractable building blocks for DCC. We demonstrated that the BDE of the dimeric form could be largely controlled by the substituent at the position *para* to the radical center. The TPA- and Cz-based diradical formed cyclic oligomers with defined sizes. We think that the three-fold symmetry of a TPA is intrinsically suited to the construction of 2D and 3D periodic structures, and the work towards realizing such structures, by self-assembly of such multiradicals, is in progress.

Acknowledgments

We deeply thank Dr. Nobuko Kanehisa (Osaka University) for help with the single-crystal X-ray analyses and Dr. Yumi Yakiyama (Osaka University) for the help on the diffuse reflectance spectroscopy measurements. This work was supported by a Grant-in-Aid for Young Scientists (B) (26810023) from the Japan Society for the Promotion of Science (JSPS) and a Grant-in-Aid for Scientific Research on Innovative Areas ("π-System Figuration" Area, 26102011). D.S. thanks the JSPS Research Fellowship for Young Scientists. The theoretical calculations were performed using the Supercomputer System of Kyoto University and Research Center for Computational Science in Okazaki (Japan).

Keywords: cyclophanes · radicals · self-assembly · substituent effects · thermochromism

How to cite: *Angew. Chem. Int. Ed.* **2016**, *55*, 8634–8638
Angew. Chem. **2016**, *128*, 8776–8780

---

[1] S. J. Rowan, S. J. Cantrill, G. R. L. Cousins, J. K. M. Sanders, J. F. Stoddart, *Angew. Chem. Int. Ed.* **2002**, *41*, 898–952; *Angew. Chem.* **2002**, *114*, 938–993.
[2] P. T. Corbett, J. Leclaire, L. Vial, K. R. West, J. L. Wietor, J. K. M. Sanders, S. Otto, *Chem. Rev.* **2006**, *106*, 3652–3711.
[3] J.-M. Lehn, *Chem. Soc. Rev.* **2007**, *36*, 151–160.
[4] Y. Jin, C. Yu, R. J. Denman, W. Zhang, *Chem. Soc. Rev.* **2013**, *42*, 6634–6654.
[5] H. D. Hartzler, *J. Org. Chem.* **1966**, *31*, 2654–2658.
[6] H. Suzuki, H. Koide, T. Ogawa, *Bull. Chem. Soc. Jpn.* **1988**, *61*, 501–504.
[7] H. A. P. de Jongh, C. R. H. I. de Jonge, W. J. Mijs, *J. Org. Chem.* **1971**, *36*, 3160–3168.
[8] H. A. P. de Jongh, C. R. H. I. de Jonge, H. J. M. Sinnige, W. J. de Klein, W. G. B. Huysmans, W. J. Mijs, *J. Org. Chem.* **1972**, *37*, 1960–1966.
[9] C. Harnack, W. Krull, M. Lehnig, W. P. Neumann, A. K. Zarkadis, *J. Chem. Soc. Perkin Trans. 2* **1994**, 1247–1252.
[10] M. Frenette, C. Aliaga, E. Font-Sanchis, J. C. Scaiano, *Org. Lett.* **2004**, *6*, 2579–2582.
[11] a) L. M. Pisarenko, V. I. Nikulin, A. B. Gagarina, *Izv. Akad. Nauk SSR Ser. Khim.* **1987**, *6*, 1237–1243; b) L. M. Pisarenko, V. I. Nikulin, I. V. Khudyakov, *Izv. Akad. Nauk SSR Ser. Khim.* **1987**, *8*, 1734–1738.
[12] L. M. Pisarenko, A. B. Gagarina, V. A. Roginskii, *Izv. Akad. Nauk SSR Ser. Khim.* **1987**, *6*, 2861–2863.
[13] J. Ohkanda, Y. Mori, K. Maeda, E. Osawa, *J. Chem. Soc. Perkin Trans. 2* **1992**, 59–63.
[14] Y. Mori, N. Yamada, M. Kanazawa, Y. Horikoshi, Y. Watanabe, K. Maeda, *Bull. Chem. Soc. Jpn.* **1996**, *69*, 2355–2359.
[15] CCDC 1471585 ($\mathbf{1_2}$), CCDC 1471587 ($\mathbf{2_2}$), CCDC 1471586 ($\mathbf{3_2}$), and CCDC 1471588 ($\mathbf{4_3}$) contain the supplementary crystallographic data for this paper. These data can be obtained free of charge from The Cambridge Crystallographic Data Centre.
[16] a) A. P. Coté, A. I. Benin, N. W. Ockwig, M. O'Keeffe, A. J. Matzger, O. M. Yaghi, *Science* **2005**, *310*, 1166–1170; b) J. W. Colson, W. R. Dichtel, *Nat. Chem.* **2013**, *5*, 453–465.
[17] D. Beaudoin, T. Maris, J. D. Wuest, *Nat. Chem.* **2013**, *5*, 830–834.

[18] G. Wittig, E. Dreher, W. Reuther, H. Weidinger, R. Steinmetz, *Justus Liebigs Ann. Chem.* **1969**, *726*, 188–200.

[19] a) J. Ipaktschi, R. Hosseinzadeh, P. Schlaf, E. Dreiseidler, R. Goddard, *Helv. Chim. Acta* **1998**, *81*, 1821–1834; b) J. Ipaktschi, R. Hosseinzadeh, P. Schlaf, *Angew. Chem. Int. Ed.* **1999**, *38*, 1658–1660; *Angew. Chem.* **1999**, *111*, 1765–1768; c) J. Ipaktschi, R. Hosseinzadeh, P. Schlaf, T. Eckert, *Helv. Chim. Acta* **2000**, *83*, 1224–1238.

[20] D. Beaudoin, O. Levasseur-Grenon, T. Maris, J. D. Wuest, *Angew. Chem. Int. Ed.* **2016**, *55*, 894–898; *Angew. Chem.* **2016**, *128*, 906–910.

[21] X. Fu, D. Zhao, *Org. Lett.* **2015**, *17*, 5694–5697.

Received: April 7, 2016